HOKKAIDO UNIVERSITY

Title	Formation of GaN porous structures with improved structural controllability by photoassisted electrochemical etching
Author(s)	Kumazaki, Yusuke; Yatabe, Zenji; Sato, Taketomo
Citation	Japanese Journal of Applied Physics (JJAP), 55(4), 04EJ12 https://doi.org/10.7567/JJAP.55.04EJ12
Issue Date	2016-04
Doc URL	https://hdl.handle.net/2115/64688
Rights	© 2016 The Japan Society of Applied Physics
Type	journal article
File Information	JJAP55_04EJ12.pdf

Hokkaido University Collection of Scholarly and Academic Papers : HUSCAP

Formation of GaN porous structures with improved structural controllability by photoassisted electrochemical etching

Yusuke Kumazaki, Zenji Yatabe, and Taketomo Sato
Research Center for Integrated Quantum Electronics, and Graduate School of Information Science and Technology, Hokkaido University, Sapporo 060-8628, Japan

ABSTRACT

We aimed to develop a photoassisted electrochemical etching process for the formation of GaN porous structures. Pore linearity and depth controllability were strongly affected by the anode voltage. In addition, the use of light with an energy below the band gap played an important role in controlling the pore diameter. Spectro-electrochemical measurements revealed that the high electric field induced at the GaN/electrolyte interface caused a redshift of the photoabsorption edge. This specific phenomenon can be explained by a theoretical calculation based on the Franz-Keldysh effect. On the basis of the results of our experimental and theoretical analyze, we propose a formation model for GaN porous structures. We also note that the application of the Franz-Keldysh effect is useful in controlling the structural properties of GaN porous structures.

Keywords: porous structure, Gallium Nitride (GaN), electrochemical etching, Franz-Keldysh effect

---

*Corresponding author. E-mail address: kumazaki@rciqe.hokudai.ac.jp

1. Introduction

Gallium nitride (GaN) and its alloys are attractive building block materials for various functional devices, such as light-emitting diodes (LEDs),[1,2] laser diodes,[3] solar cells,[4] and so on.[5,6] One promising approach for improving device performance is the formation of nanostructures with unique physical and optical features. Most reported GaN nanostructures have been formed using a selective-area growth[7,8] or dry etching process such as reactive-ion etching (RIE).[9,10] There are, however, severe limitations on increasing the density of nanostructures, because most approaches use lithography to define the size and position of the nanostructures. Furthermore, when a dry etching process is involved, the etching damage induced by ion bombardment is considerable[11-13] and could significantly degrade the device performance.

One alternative approach is an electrochemical fabrication process, which can form various semiconductor nanostructures in a self-assembled fashion. The most well-known application of such an electrochemical process is the formation of porous structures by anodic etching, in which a high-density array of nanometer- or micrometer-sized pores is formed with high productivity over a large area on the semiconductor surface.[14-18] In addition, optical properties are significantly enhanced by the formation of porous structures.[19,20] These features are very promising for use in functional devices mentioned above.

The electrochemical conditions including applied bias and electrolyte solutions have been investigated with regard to the formation of GaN porous structures.[21] Thus far, however, the controllability of structural properties such as the pore diameter and depth has been inadequate.[22,23] One reason for the difficulty in structural control is that a photoassisted electrochemical process is commonly used, and this formation process becomes more complicated as the illumination generates a supply of photocarriers.[24]

In this study, therefore, we aimed to develop a photoassisted electrochemical etching process for forming GaN porous structures with better structural controllability. Spectro-electrochemical measurements were also conducted to clarify the relationship between photoabsorption and the electrochemical reaction.

2. Methods

An n-type GaN substrate (N_D = 1 × 10^{18} cm^{-3}) with a thickness of 400 μm was used in this study. Gold (Au) was deposited at one corner of the back surface to supply an electrochemical current. A custom-made electrochemical cell was used to form porous structures and conduct spectro-electrochemical measurements, as shown schematically in Fig. 1. The electrochemical cell consisted of three electrodes: an n-type GaN working electrode (WE), a Pt counter electrode (CE), and a Ag/AgCl reference electrode (RE). We used a mixture of 1 mol/L H_2SO_4 and 1 mol/L H_3PO_4 as an electrolyte. The GaN porous structures were formed under various

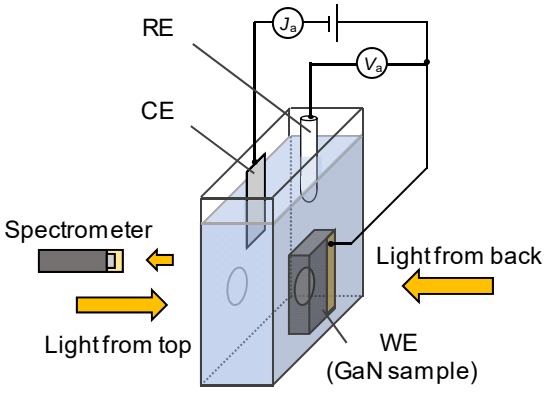

Fig. 1. Schematic illustration of the electrochemical setup used for both the formation of porous structures and the spectro-electrochemical measurements.

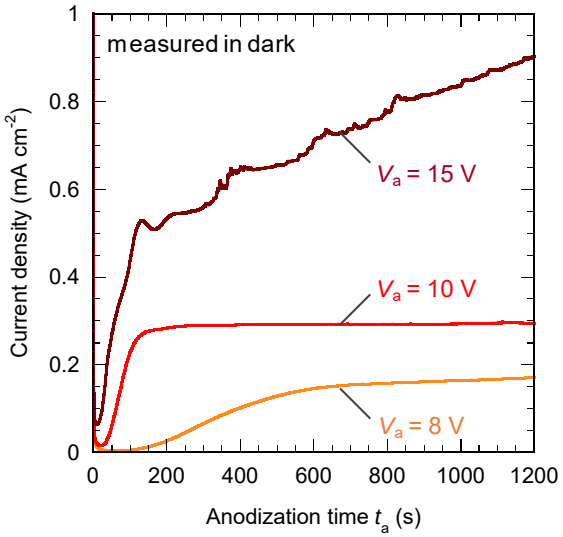

Fig. 2. Current-time curves obtained during anodization at various anode voltage V_a values.

electrochemical conditions by varying such parameters as the anode voltage V_a, anodization time t_a, and light conditions. A xenon (Xe) lamp with an optical filter was used as the light source. The structural properties of the porous structures were evaluated by scanning electron microscopy (SEM) with a Hitachi SU-8010 system. The spectro-electrochemical properties were evaluated by measuring the transmittance of light irradiated from the back surface with an Ocean Optics HR4000CG-UV-NIR spectrometer, under a voltage applied in the same setup shown in Fig. 1.

3. Results and discussion

3.1 Formation of GaN porous structures

Before applying the photoassisted electrochemical process, the anode voltage condition was first optimized in the dark. Figure 2 shows current-time curves obtained during anodization at various anode voltage V_a values. At the initial stage of electrochemical reactions, anodic currents increased for one hundred seconds or more. The slope of the curve increased with V_a; in other words, the reaction rate increased with V_a. In addition, we found that anodic currents saturated for the data obtained at V_a = 8 and 10 V, but they kept increasing at V_a = 15 V. These results indicate that the reaction rates at V_a = 8 and 10 V become constant after one hundred seconds, whereas the reaction rate at V_a = 15 V increases with anodization time.

Figures 3(a)-(c) show SEM images of GaN porous structures formed with t_a = 1200 s and various anode voltages: (a) V_a = 8 V, (b) V_a = 10 V, and (c) V_a = 15 V. The sample formed at V_a = 8 V [Fig. 3(a)] had straight pores oriented perpendicular to the top surface, with pores branching from the straight pores. The sample formed at V_a = 10 V [Fig. 3(b)] also had straight pores oriented perpendicular to the top surface, but the pore branching observed at V_a = 8 V was significantly suppressed. The pore diameter and depth were estimated as approximately 16 nm and 1.3 μm, respectively, throughout the entire porous region. The general features observed here can be roughly explained in terms of two different, competing processes. The first process is pore formation in the preferential directions of weak bonds that are easily attacked by the electrolyte. The second

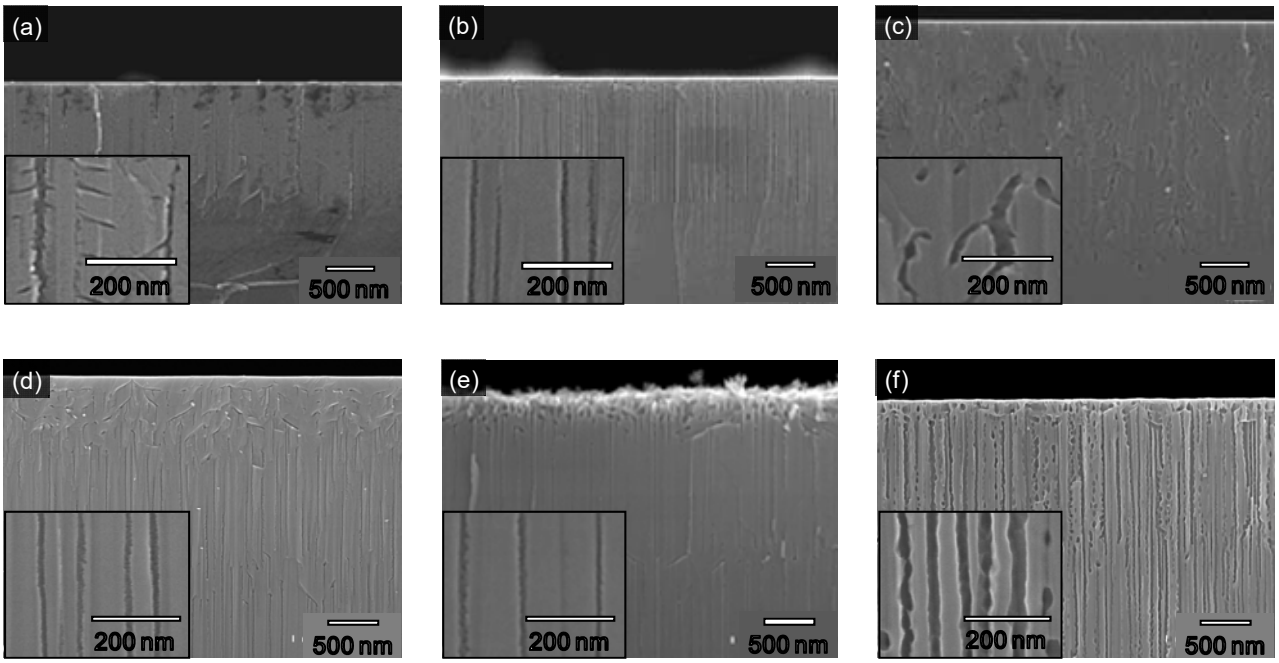

Fig. 3. Cross-sectional SEM images of GaN porous structures formed under various electrochemical conditions: (a) dark, t_a = 1200 s, V_a = 8 V; (b) dark, t_a = 1200 s, V_a = 10 V; (c) dark, t_a = 1200 s, V_a = 15 V; (d) dark, t_a = 2400 s, V_a = 10 V; (e) illuminated, t_a = 2400 s, V_a = 10 V, $h\nu$ = 3.54 eV; (f) illuminated, t_a = 2400 s, V_a = 10 V, $h\nu$ = 3.26 eV.

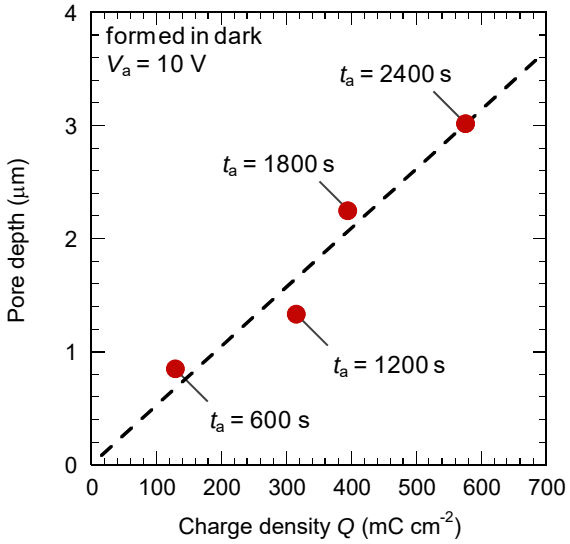

Fig. 4. Relationship between pore depth and density of charges, Q, passing through the working electrode during electrochemical etching.

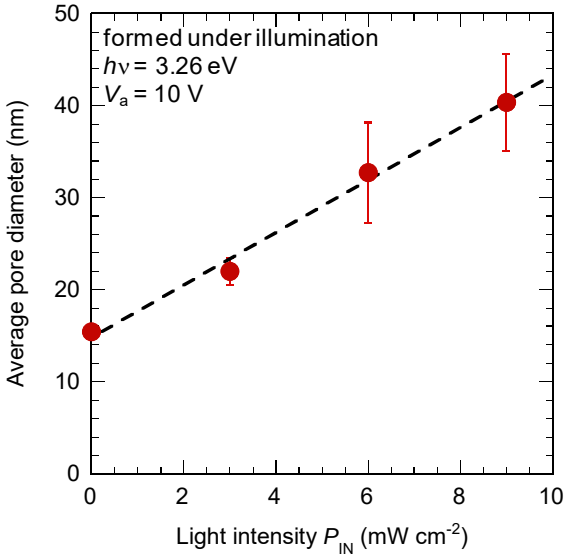

Fig. 5. Relationship between pore diameter and light intensity P_{IN} with $h\nu$ = 3.26 eV.

process is the formation of straight pores along the direction of the electric field producing the holes required for the etching reaction. This tendency is enhanced at higher anodization voltages, as in the case of InP porous structures formed in the dark.[25] On the other hand, the pores formed at V_a = 15 V [Fig. 3(c)] had diminished linearity and size uniformity. This was probably because the lateral etching of the pore walls was enhanced by the generation of holes in the walls. From these results, we can conclude that pore morphologies are markedly affected by V_a, and that electrochemical etching at V_a = 10 V can achieve the formation of linear, uniform porous structures.

Figure 3(d) shows an SEM image of GaN porous structures formed with t_a = 2400 s and V_a = 10 V. As compared with those of the sample shown in Fig. 3(b), the pore diameter and linearity of the structures shown in Fig. 3 remained unchanged, but the pore depth increased with t_a. Figure 4 shows the relationship between pore depth and the density of charges, Q, passing through the working electrode during anodization. We found that the pore depth increased linearly with Q. Considering the proportional relationship between the amount of electrochemical reaction and Q, as described by Faraday's law, the electric charges contributed only to vertical etching, resulting in superior depth controllability. The pore diameter, however, could not be controlled throughout the electrochemical etching in the dark.

To investigate the feasibility of diameter control, the photoassisted electrochemical etching was next conducted in the front-side illumination mode. Figures 3(e) and 3(f) show SEM images of GaN porous structures formed at V_a = 10 V and t_a = 2400 s, under monochromatic light with energy $h\nu$ values of (e) 3.54 and (f) 3.26 eV. Under illumination with $h\nu$ = 3.54 eV, which is larger than the band gap E_g of GaN, only pores near the top surface were affected by the light. In other words, the pore diameter increased only in the top region, to a depth of about 200 nm, as compared with that of the samples formed in the dark. From SEM observations, an average pore diameter of 50 nm was obtained in the top region, which is approximately 30 nm larger than the pore diameter in the deeper region. On the other hand, under illumination with $h\nu$ = 3.26 eV (< E_g), the pore diameter increased to approximately 40 nm throughout the entire porous layer. Figure 5 shows the average pore diameter plotted as a function of the light intensity P_{IN}. We found that the pore diameter increased linearly with P_{IN}. These results clearly indicate that using light with $h\nu$ below the band gap of GaN enables the tuning of the diameter without diminishing the linearity or depth controllability of the pores.

3.2 Spectro-electrochemical properties

To clarify how the photoabsorption process affects electrochemical reactions, spectro-electrochemical measurements were conducted on planar GaN substrates. Figure 6(a) shows transmittance spectra for T_{0V} and T_{10V} obtained by applying anode voltages of V_a = 0 and 10 V, respectively, in the electrochemical setup shown in Fig. 1. We could observe a strong dependence of the transmittance on V_a at around 3.3 eV. The transmittance difference T_{0V} - T_{10V} is plotted in Fig. 6(b) as a function of the photon energy $h\nu$. The difference was almost zero at energies higher than E_g because of absorption by the bulk GaN. On the other hand, larger differences could be observed at energies below E_g, reaching a maximum at around 3.3 eV and decreasing as $h\nu$ decreased . These results indicate that photoabsorption near the band edge can be enhanced by the electric field mostly applied at the GaN/electrolyte interface.

One possible phenomenon to explain the above results is the Franz-Keldysh effect, which causes the redshift of the absorption edge under a high electric field, leading to the occurrence of absorption below the bulk band gap E_g.[26,27] Generally, a high electric field is applied

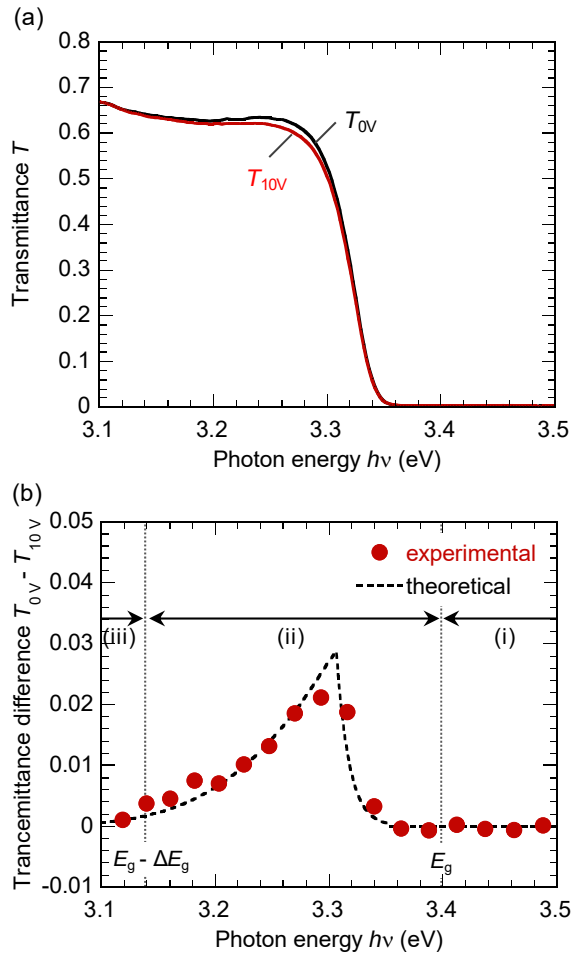

Fig. 6. (a) Transmittance spectra of a GaN planar electrode, obtained by applying anode voltages of V_a = 0 and 10 V in the electrochemical setup shown in Fig. 1. (b) Transmittance difference T_{0V} - T_{10V} plotted as a function of the photon energy $h\nu$.

by the formation of a potential barrier of about 1.0 eV at the GaN/electrolyte interface.[28,29] When the doping density is as high as 10^{18} cm^{-3}, for example, the internal electric field in a thin depletion layer with a width of several dozen nanometers reaches 5×10^5 V/cm. In such a situation, the electron and hole wave functions become Airy functions, which extend into the band gap, enabling band-to-band transition at energies below E_g. In the depletion region, the Franz-Keldysh relative absorption coefficient α can be approximated as[30,31]

$$\alpha \sim \alpha_0 \exp\left(-\left|\frac{h\nu - E_g}{\Delta E_g}\right|^{\frac{3}{2}}\right). \quad (1)$$

Here, α_0 is the absorption coefficient at $h\nu = E_g$, and ΔE_g is the redshift energy of the absorption edge, expressed by

$$\Delta E_g = \frac{2}{3}\frac{(e\hbar\xi)^{\frac{3}{2}}}{(m^*)^{\frac{1}{3}}}, \quad (2)$$

where q, $\hbar$, ξ, and m^* are the elementary charge, Dirac's constant, electric field, and effective mass, respectively. The transmittance T is expressed as a function of the reflectance R, absorption coefficient α, and optical path length x, as follows:

$$T = (1-R)\exp(-\alpha x). \quad (3)$$

Through calculations using Eqs. (1)-(3), we estimated the transmittance difference T_{0V} - T_{10V}, plotted in Fig. 6(b) with a dotted line. The experimental data are very consistent with the prediction of the Franz-Keldysh effect. In the case of illumination with $h\nu > E_g$ [case (i)], T_{0V} - T_{10V} was almost zero since all photons were absorbed near the surface. For illumination with E_g - ΔE_g < $h\nu$ < E_g [case (ii)], the photons penetrated through the bulk GaN but were absorbed at the GaN/electrolyte interface only under a high electric field because of the Franz-Keldysh effect. In that situation, T_{0V} - T_{10V} increased up to an observable level, as shown in Fig. 6(b). Finally, for illumination with $h\nu < E_g$ - ΔE_g [case (iii)], since photons were not absorbed either in the bulk GaN or at the GaN/electrolyte interface, T_{0V} - T_{10V} decreased again. These results suggest that light with E_g - ΔE_g < $h\nu$ < E_g plays an important role in the photoassisted electrochemical process.

3.3 Formation mechanism of GaN porous structures

To investigate the possibility of applying the Franz-Keldysh effect, we calculated the potential distribution of GaN porous structures in an electrolyte by solving a 3D Poisson equation. Figure 7(a) shows the potential distribution of the conduction band minimum measured from the Fermi level, E_C - E_F, with the solid lines indicating contours at 0.2, 0.4, 0.6, 0.8, and 1.0 eV. The pore pitch, depth, and potential difference between the GaN and electrolyte were specified as 25 nm, 50 nm, and 1.0 eV, respectively. Although no external voltage is applied, the potential distribution is strongly modified near the pore tips, where the contour intervals become narrow. Figure 7(b) shows cross-sectional potential distributions obtained at the top surface (line i) and pore tips (line ii). The potential variation at the pore tips is much larger than that at the top surface, reflecting the high electric field applied to the tips.

On the basis of the above discussion, we propose a formation model for GaN porous structures. For formation in the dark, the electrochemical etching is performed by the carriers generated by the avalanche effect induced by the concentrated electric field at the pore tips. Since the electric fields at the pore walls and top surface are small, the electrochemical etching proceeds only in the depth direction at the pore tips. That is why the process of forming GaN porous structures in the dark can achieve superior linearity and depth controllability but cannot vary the pore diameter. Under illumination with $h\nu > E_g$, photons are preferentially absorbed near the top surface because of band-edge absorption. Photogenerated carriers are then transferred to the top surface and pore walls by the electric field, and

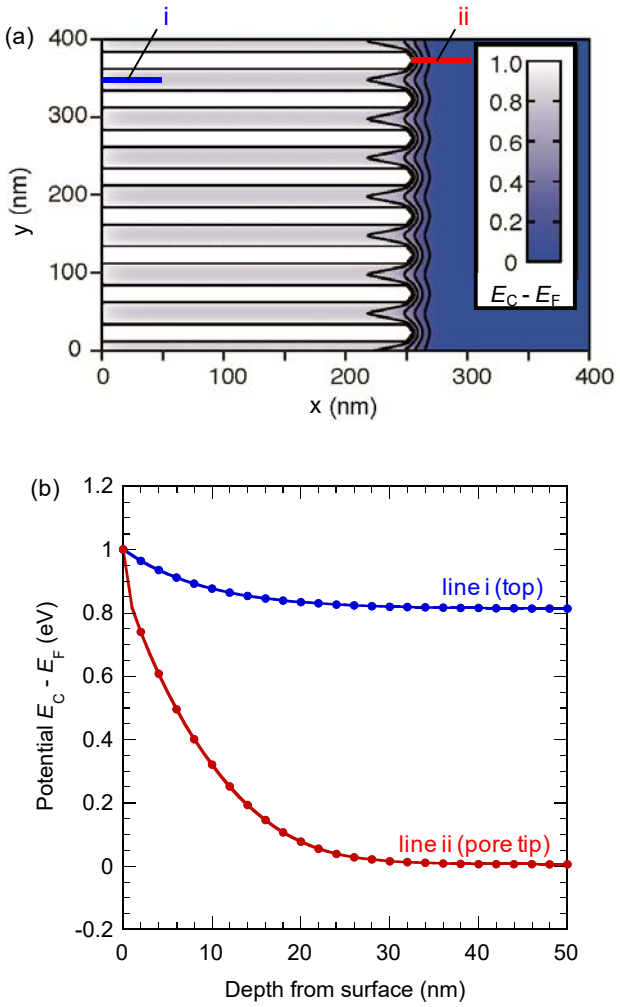

Fig. 7. (a) Potential distribution in GaN porous structures drawn with contour levels at 0.2. 0.4, 0.6, 0.8, and 1.0 eV, and (b) the cross-sectional potential distribution at the top surface (line i) and pore tips (line ii) obtained by solving 3D Poisson equation.

contribute to the electrochemical etching. This explains the larger pore region with a thickness of 200 nm, a value consistent with the light penetration depth in GaN [see Fig. 3(e)]. Under illumination with E_g - ΔE_g < $h\nu$ < E_g, however, photons are transmitted in the top region but absorbed only at the pore tips where a high electric field is applied. In this situation, the photocarriers generated by the Franz-Keldysh effect are consumed at the pore tips and assist the electrochemical etching. As seen from Fig. 5, in fact, the pore diameter increased with the light intensity, as the number of carriers contributing to the electrochemical etching increased. This formation model can consistently explain both the experimental results and the theoretical model, enabling us to conclude that the application of the Franz-Keldysh effect is useful in controlling the structural properties of GaN porous structures.

4. Conclusions

Porous structures in GaN were formed by electrochemical etching under various conditions. Pore linearity and depth controllability were improved by selecting an appropriate anode voltage V_a. In addition, we succeeded in controlling the pore diameter by using light with $h\nu$ below the band gap. Spectro-electrochemical measurements revealed that the high electric field induced at the GaN/electrolyte interface caused a redshift of the photoabsorption edge. This specific phenomenon could be consistently explained by a theoretical calculation based on the Franz-Keldysh effect. On the basis of the results of our experimental and theoretical analyze, we proposed a formation model for GaN porous structures. We also concluded that the application of the Franz-Keldysh effect is useful in controlling the structural properties of GaN porous structures.

Acknowledgement

This work was supported in part by a Grant-in-Aid for JSPS Fellows 14J01371, a Grant-in-Aid for Scientific Research (B) 25289079, and a Grant-in-Aid for Challenging Exploratory Research 15K13937, from the Japan Society for the Promotion of Science (JSPS).

References

1) S. Nakamura, T. Mukai, and M. Senoh, Jpn. J. Appl. Phys. **30**, L1998 (1991).
2) I. Akasaki and H. Amano, Jpn. J. Appl. Phys. **45**, 9001 (2006)
3) S. Nakamura, M. Senoh, S. Nagahara, N. Iwasa, T. Yamada, T. Matsushita, H. Kiyoku, and Y. Sugimoto, Jpn. J. Appl. Phys. **35**, L74 (1996)
4) C. J. Neufeld, N. G. Toledo, S. C. Cruz, M. Iza, S. P. DenBaars, and U. K. Mishra, Appl. Phys. Lett. **93**, 143502 (2008).
5) K. Fujii, T. Karasawa, and K. Ohkawa, Jpn. J. Appl. Phys. **44**, L543 (2005).
6) S. Yotsuhashi, M. Deguchi, Y. Zenitani, R. Hinogami, H. Hashiba, Y. Yamada, and K. Ohkawa, Appl. Phys. Express **4**, 117101 (2011).
7) Y. D. Wang, K. Y. Zang, and S. J. Chua, J. Appl. Phys. **100**, 054306 (2006).
8) I. Waki, D. Cohen, R. Lal, U. Mishra, S. P. DenBaars, and S. Nakamura, Appl. Phys. Lett. **91**, 093519 (2007).
9) H. Ono, Y. Ono, K. Kasahara, J. Mizuno, and S. Shoji, Jpn. J. Appl. Phys. **47**, 933 (2008).
10) W. M. Zhou, G. Q. Min, Z. T. Song, J. Zhang, Y. B. Liu, and J. P. Zhang, Nanotechnology **21**, 205304 (2010).
11) E. D. Haberer, C. H. Chen, A. Abare, M. Hansen, S. Denbaars, L. Coldren, U. Mishra, and E. L. Hu, Appl. Phys. Lett. **76**, 3941 (2000).
12) R. Dimitrov, V. Tilak, W. Yeo, B. Green, H. Kim, J. Smart, E. Chumbes, J. R. Shealy, W. Schaff, L. F. Eastman, C. Miskys, O. Ambacher, and M. Stutzmann, Solid-State Electron. **44**, 1361 (2000).
13) F. A. Khan, L. Zhou, V. Kumar, and I. Adesida, J. Vac. Sci. Technol. B **19**, 2926 (2001).
14) A. Uhlir, Bell Syst. Tech. J. **35**, 333 (1956).
15) V. Lehmann, J. Electrochem. Soc. **140**, 2836 (1993).
16) B. H. Erné, D. Vanmaekelbergh, and J. J. Kelly, J. Electrochem. Soc. **143**, 305 (1996).
17) H. Hasegawa and T. Sato, Electrochim. Acta **50**, 3015

(2005).
18) H. Asoh, K. Nishio, M. Nakao, T. Tamamura, and H. Masuda, J. Electrochem. Soc. **148**, B152 (2001).
19) T. Sato, N. Yoshizawa, and T. Hashizume, Thin Solid Films **518**, 4399 (2010).
20) Y. Kumazaki, T. Kudo, Z. Yatabe, and T. Sato, Appl. Surf. Sci. **279**, 116 (2013).
21) S. F. Cheah, S. C. Lee, S. S. Ng, F. K. Yam, H. Abu Hassan, and Z. Hassan, J. Lumin. **159**, 303 (2015).
22) W. J. Tseng, D. H. van Dorp, R. R. Lieten, P. M. Vereecken, and G. Borghs, J. Phys. Chem. C **118**, 29492 (2014).
23) Y. Kumazaki, A. Watanabe, Z. Yatabe, and T. Sato, J. Electrochem. Soc. **161**, H705 (2014).
24) A. Watanabe, Y. Kumazaki, Z. Yatabe, and T. Sato, ECS Electrochem. Lett. **4**, H11 (2015).
25) T. Sato, T. Fujino, and H. Hasegawa, Appl. Surf. Sci. **252**, 5457 (2006).
26) W. Franz, Z. Naturforsch. A **13**, 484 (1958).
27) L. V. Keldysh, Sov. Phys. JETP **6**, 763 (1958).
28) S. S. Kocha, M. W. Peterson, D. J. Arent, J. M. Redwing, M. A. Tischler, and J. A. Turner, J. Electrochem. Soc. **142**, L238 (1995).
29) I. M. Huygens, K. Strubbe, and W. P. Gomes, J. Electrochem. Soc. **147**, 1797 (2000).
30) H. Y. Peng, M. D. McCluskey, Y. M. Gupta, M. Kneissl, and N. M. Johnson, Appl. Phys. Lett. **82**, 2085 (2003).
31) A. Cavallini, L. Polenta, and M. Rossi, Nano Lett. **7**, 2166 (2007).